Yonsei Med J 49(6):965 - 972, 2008
DOI 10.3349/ymj.2008.49.6.965

Point Mutation of Hoxd12 in Mice

Kyoung-Won Cho,[1] Jae-Young Kim,[2] Jae-Woo Cho,[3] Kyu-Hyuk Cho,[3] Chang-Woo Song,[3] and Han-Sung Jung[1]

[1]Division in Anatomy and Developmental Biology, Department of Oral Biology, Research Center for Orofacial Hard Tissue Regeneration, Brain Korea 21 Project, Oral Science Research Center, College of Dentistry, Yonsei Center of Biotechnology, Yonsei University, Seoul; [2]Department of Biochemistry, School of Dentistry, Kyungpook National University, Daegu; [3]Laboratory of Toxicogenomics, Korea Institute of Toxicology, Korea Research Institute of Chemical Technology, Deajeon, Korea.

Purpose: Genes of the HoxD cluster play a major role in vertebrate limb development, and changes that modify the Hoxd12 locus affect other genes also, suggesting that HoxD function is coordinated by a control mechanism involving multiple genes during limb morphogenesis. In this study, mutant phenotypes were produced by treatment of mice with a chemical mutagen, N-ethyl-N-nitrosourea (ENU). We analyzed mutant mice exhibiting the specific microdactyly phenotype and examined the genes affected. **Materials and Methods:** We focused on phenotype characteristics including size, bone formation, and digit morphology of ENU-induced microdactyly mice. The expressions of several molecules were analyzed by genome-wide screening and quantitative real-time PCR to define the affected genes. **Results:** We report on limb phenotypes of an ENU-induced A-to-C mutation in the Hoxd12 gene, resulting in alanine-to-serine conversion. Microdactyly mice exhibited growth defects in the zeugopod and autopod, shortening of digits, a missing tip of digit I, limb growth affected, and dramatic increases in the expressions of Fgf4 and Lmx1b. However, the expression level of Shh was not changed in Hoxd12 point mutated mice. **Conclusion:** These results suggest that point mutation rather than the entire deletion of Hoxd12, such as in knockout and transgenic mice, causes the abnormal limb phenotype in microdactyly mice. The precise nature of the spectrum of differences requires further investigation.

Key Words: N-ethyl-N-nitrosourea induced mice, microdactyly, Hoxd12, limb and digit abnormality, point mutation

Received April 2, 2008
Accepted June 4, 2008

This work was supported by the Korea Science and Engineering Foundation (KOSEF) grant funded by the Korea government (MEST) (No. R13-2003-013-05001-0).

Reprint address: requests to Dr. Han-Sung Jung, Division in Anatomy and Developmental Biology, Department of Oral Biology, College of Dentistry, Yonsei University, 250 Seongsanno, Seodaemun-gu, Seoul 120-752, Korea. Tel: 82-2-2228-3064, Fax: 82-2-312-8012, E-mail: hsjung@yuhs.ac

INTRODUCTION

Understanding genes that function in the pathogenesis of human disease is essential for developing effective diagnoses and therapies, and animal models are indispensable tools for studying gene function. N-ethyl-N-nitrosourea (ENU) is a powerful spermatogonial mutagen that induces one point mutation per million base pairs in laboratory mice.[1] Several research centers are conducting large-scale screening programs for producing novel ENU-induced mutants that model human disease.[2] The point mutagenicity induced by ENU potentially allows for the identification of multiple allelic variants at each gene locus that lead to complete loss of gene function (null allele), partial loss of function (hypomorphic), gain of function (hypermorphic), dominant negative function (antimorphic), or novel gain of function (neomorphic).[3] Screening for ENU mutagenesis is phenotype-driven, and is a powerful way to identify gene function due to the absence of a prior assumptions.

The vertebrate limb is an ideal model system for studying signaling mechanisms and pattern formation.[4,5] Signaling by the polarizing region expressing Shh establishes both the number and characteristics of the digits that can be temporally uncoupled.[6-9]

Hox genes are divided into 4 linkage groups (called Hoxa, -b, -c, and d) that are essential for the development of limb extremities. Hoxd12 differentially affects the paraxial and postaxial chondrogenic branching in the limb, and regulates Shh in a positive feedback loop.[10] Moreover, studies of the Hoxd12 regulatory elements have revealed global and local control elements of the

Hoxd complex.[11] Hoxd expression data suggest that the most anterior digit in a bird wing is homologous to digit 1 (and not digit 2) in other amniotes.[12,13]

In this study, we carried out both genome-wide screening and point mutant screening to identify the affected gene. A new ENU-generated mouse mutant exhibited microdactyly on the fore and hind limbs as a recessive trait, however appeared normal otherwise. This study fell short in establishing a strong correlation between the point mutation identified and the microdactyly phenotype observed. Positional cloning allowed the point mutated gene in Hoxd12 to be identified. We also found that Lmx1b and Fgf4 were significantly up-regulated in their mutant mouse line. The present observation would be of potential interest for the understanding of the function of Hox genes in digit development.

MATERIALS AND METHODS

All experiments were performed according to the guidelines of the Yonsei University, College of Dentistry, Intramural Animal Use and Care Committee.

Animals

Mice were obtained from Charles River, Japan. All mice were maintained in the barrier system under specific-pathogen-free conditions with regulated light (07:00 - 19:00 hours), temperature (23 ± 1 °C), humidity (50 ± 5%), and ventilation (10 - 12 times per hour). The care and treatment of the animals was in accordance with the Guide for the Care and Use of Laboratory Animals (NIH). All animal experiments were approved by the Institutional Animal Care and Use Committee of the Korea Research Institute of Chemical Technology. All experiments were carried out in accordance with the Guidelines for Animal Experimentation. The BALB/cJ male mice were intraperitoneally injected twice with ENU (100 mg/kg), 2 weeks apart. Using a 3-generation breeding scheme, an ENU induced microdactyly was established as a mutant strain.

Skeletal staining

For skeletal analyses, mice were collected at 8 weeks. The mutant and wild type (BALB/cJ) mice were processed and stained with Alcian Blue-Alizarin Red Skeletal Staining.

Genetic mapping

To genetically map the limb mutant locus, intraspecific progenies were generated. A mutant (Mt) mouse was mated with C57BL/6 (B6) mouse. The F1 progeny of the (Mt × B6) mating were crossed with [(F1 × Mt) F2] and produced Mt mouse. Twenty one Mt progeny were used for mapping. The genetic markers were obtained from Mouse Genome Informatics (Blake et al. 2003). Two polymorphic microsatellite markers (D2Mit329 and D2Mit285) were used for linkage analysis using standard techniques. Briefly, genomic DNA was extracted from tails according to the manufacturer's protocols (QIAamp Tissue Kit; Qiagen, Inc., Santa Clarita, CA, USA). Amplifications by polymerase chain reaction (PCR) were performed according to standard protocols. Primers were purchased from Bioneer, Inc. (Daejeon, Korea). Genetic linkage was assessed by segregation analysis. The statistical significance of the recombination was determined by $\times 2$ analysis.[14]

Mutation analysis

Genomic DNA was prepared from the liver of wild-type (WT) and homozygous mutant mice by the standard protocol and used as the template for PCR. Primer pairs were generated to GenBank (www.ncbi.nlm.nih.gov). PCR was performed in a 20 μL reaction mixture containing 25 ng of template DNA, 1× Taq buffer, 1.5 mM $MgCl_2$, 200 μM dNTPs, 0.2 μM each of primer, and 1 U of Taq polymerase (Superbio, Suwon, Korea). PCR products were purified with a Qiagen purification kit (Qiagen, Inc., Valencia, CA, USA) and sequenced using the ABI Prism BigDye Terminator Cycle Sequencing Ready Reaction Kit version 1.1 and a sequencer, ABI Model 3100 (Applied Biosystems, Foster City, CA, USA). The PCR product was digested, and DNA fragments were separated on a 12% polyacrylamide gel with 1 × TBE buffer.

Quantitative real-time PCR (RT-qPCR)

RNA was extracted from the skin of WT and homozygous mutant mice using a total RNA isolation procedure according to the manufacturer's recommendations and further purified using the WelPrep™ Total RNA isolation reagent (WelGENE, Daegu, Korea). For cDNA synthesis, reverse transcription of RNA was performed using the Revert Aid™ M-MiLV Reverse Transcriptase (Fermentas, Burlington, Ontario, Canada). Real-time PCR was performed using a Thermal Cycler Dice™ Real Time System (Takara, Shiga, Japan) according to the manufacturer's instructions. Reverse transcriptase and buffer were from SYBR Premix EX Taq™ (Perfect Real Time, Takara, Shiga, Japan). The PCR for each sample was performed in triplicate, and the amounts of the PCR products were normalized using GAPDH as an internal control. The data were analyzed with the Thermal Cycler Dice™ Real Time System analysis software (Takara TP800, Shiga, Japan). To determine the relative level of gene expression, we used the comparative ΔΔCt method, previously described by Livak and Schmittgen. The Student t-test was employed to determine significant changes at the 95% confidence level ($*p < 0.01$).

RESULTS

ENU-induced microdactyly mice

Recessive mutagenesis screening produced ENU-induced microdactyly mice at the third generation that could be distinguished from their normal littermates at birth. Both wild-type (WT) and mutant mice had five digits on the fore and hind limbs, and our mutant mice did not show the syndactyly or polydactyly phenotype (Fig. 1).

WT and heterozygous mice appeared identical at birth, showing normal growth and limb development. In contrast, however, homozygous mutants induced by ENU were characterized by small limbs and digits at birth, whereas other organs such as kidney and lung appeared to be normal (data not shown). Skeletal analysis of microdactyly mice showed additional abnormalities in the radius (R), ulna (U), tibia (T), and fibula (F) (Figs. 1e, f, q, and r). Microdactyly mice had widely expanded digits, and digit I was shorter than those in WT mice (Figs. 1a-d, i, and j). Only digit IV was unaffected on the fore limb (Figs. 1a-d), and the tip of digit I was missing in microdactyly mice (Figs. 1a, g, and j). All the phalanges of digit V were shorter in microdactyly mice than in WT mice (Figs. 1a, b, h, and k), especially for the metacarpal bone (first phalange: microdactyly, 0.1 cm; WT, 0.2 cm, Table 1) and medial phalanx (third phalange: microdactyly, 0.1-cm; WT, 0.2 cm, Table 1), which were half the length of those in WT mice (Figs. 1a, b, i, and l). In addition, both the radius and ulna were smaller and misshapen in microdactyly mice (Figs. 1e and f); specifically, the bones were thinner and the interosseous space of fore limb was wider than in WT mice, although the total length (1.3 cm, Table 1) was the same (Figs. 1e and f).

The microdactyly hind limb had abnormal digits at birth, with the limbs also being shorter than in WT mice (Figs. 1m-p). Although no phalanges were missing, the abnormalities were more significant than in the fore limbs (Figs. 1a-d and m-p). Digits I, II, and V were more curved than normal digits (Figs. 1m-x). Moreover, all the first phalanges were shorter and thicker, and all the joints were thicker in microdactyly mice than in WT mice (Figs. 1m, o, and s-z). The metatarsal bone of digit I was shorter than normal, and was not connected properly to the end of the metatarsal bone. The digital phalanx (tip) was normal (Figs. 1m, o, s, and v). Similar to digit I, digit II of the metatarsal bone was also shorter, thicker, and curved, and also showed a hind limb abnormality (Figs. 1m, o, t, w, y, and z). The proximal phalanx of digit II was thinner in microdactyly mice than in WT mice, and the middle phalanx was bent proximally (Figs. 1m and o). Digit V of microdactyly mice was also curved proximally, and therefore the space between digits IV and V was larger than in WT mice (Figs. 1m-p, v, and x-z). Microdactyly mice exhibited abnormalities in the tibia and fibula of the hind limb, with the interosseous space being narrower than normal (Figs. 1q and r).

Point mutation of Hoxd12

To identify the mutated gene, mutant (BALB/cJ) mice were crossed with C57BL/6 mice, and

Table 1. Lenght of Digit and Limb

		Fore limb		Hind limb	
		Microdactyly	Wild type	Microdactyly	Wild type
Ulnar		1.3	1.3	-	-
Tibia		-	-	1.9	2.1
Digit I	Phalange I	0.2	0.2	0.5	0.6
	Phalange II	0.1	0.1	0.2	0.2
	Phalange III	0.1	0.1	0.1	0.1
	Phalange IV	-	-	-	-
	Total length	0.4	0.4	0.8	0.9
Digit II	Phalange I	0.2	0.2	0.4	0.8
	Phalange II	0.2	0.2	0.4	0.4
	Phalange III	0.1	0.1	0.1	0.2
	Phalange IV	0.1	0.1	0.1	0.1
	Total length	0.6	0.6	1	1.5
Digit III	Phalange I	0.4	0.4	0.7	0.9
	Phalange II	0.2	0.2	0.4	0.4
	Phalange III	0.1	0.1	0.2	0.2
	Phalange IV	0.1	0.1	0.1	0.1
	Total length	0.8	0.8	1.4	1.6
Digit IV	Phalange I	0.4	0.4	0.7	0.9
	Phalange II	0.2	0.2	0.4	0.4
	Phalange III	0.1	0.1	0.2	0.2
	Phalange IV	0.1	0.1	0.1	0.1
	Total length	0.8	0.8	1.4	1.6
Digit V	Phalange I	0.1	0.2	0.5	0.6
	Phalange II	0.2	0.2	0.2	0.2
	Phalange III	0.1	0.2	0.1	0.1
	Phalange IV	0.1	0.1	-	-
	Total length	0.5	0.7	0.8	0.9

All values are centimeters.

the (mutant × B6) F1 was crossed with (F1 × F1) F2 to produce ENU-induced microdactyly mice. Twenty one microdactyly offspring were genotyped for linkage analysis. Among the loci associated with the microdactyly phenotype, we chose the Hoxd locus as the candidate mutant gene, based on the phenotypic similarity of mutant mice to ENU-induced microdactyly mice. The genotypes of the F2 mice are summarized in Fig. 2a. The order of the markers was centromere-D2Mit329 and D2Mit 285 (Fig. 2a), and the Hoxd cluster was located between D2Mit329 and D2Mit 285 on chromosome 2. Therefore, to identify the point mutation, we directly sequenced the Hoxd cluster in ENU-induced microdactyly mice (Fig. 2b). The sequences were determined using BLAST

searches, and weidentified a G-to-T transition at nucleotide 1359 that cosegregated with the mutant phenotype. This mutation had alanine changed to serine at the residue 453 in Hoxd12 (Fig. 2c).

Alteration patterns of significant molecules in microdactyly mice

After identifying the mutated gene, we used quantitative real-time PCR to explore the functional consequences of the Hoxd12 point mutation on limb development. These analyses were performed on 8-week-old mice. The gene-specific primers used are listed in Table 2. Compared to WT mice, the mRNA expression of Hoxd12 in ENU-mutated microdactyly mice was not altered (data not shown), whereas that of Bmp2 was moderately increased, Fgf4 and Lmx1b were dramatically increased, and Bmp4, En1, Fgf8, Ptch1, and Shh were slightly decreased (Fig. 3). Expres

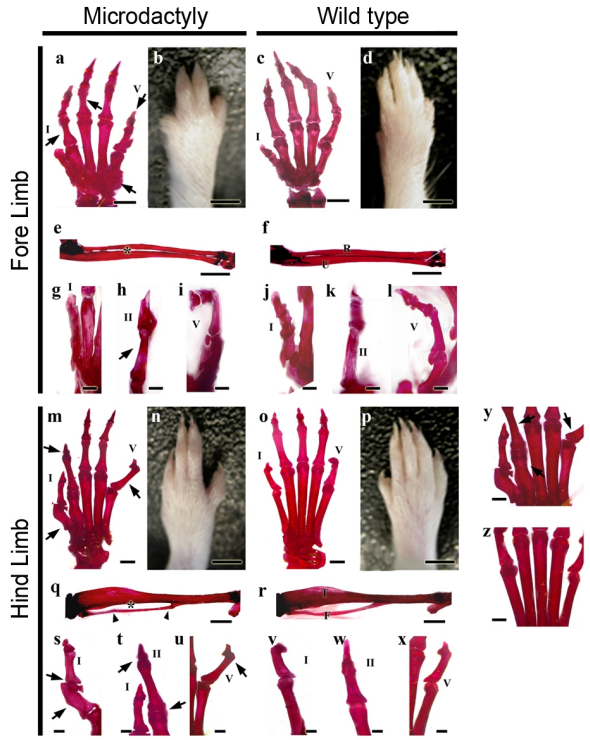

Fig. 1. Dorsal views of fore (a-l) and hind (m-z) limbs of ENU-induced microdactyly and WT (BALB/cJ) mice. Digits I, II, III, and V were shorter in microdactyly than in WT mice, and were curved, with only digit IV being the same in the fore limb (a-d). Digit I was widely expanded and shorter in microdactyly than in WT mice (a, c, g, and j). Compared with WT mice, the tip of digit I was missing in microdactyly mice (a, g, and j), the radius and ulna were shorter and thinner (e and f), the interosseous space of the fore limb was larger, all first phalanges were shorter and thicker, all joints were thicker (m, o, and s-z), and the metatarsal of digit I was shorter, whereas the digital phalanx (tip) was normal (m, o, and s). In digit II, the metatarsal bone was shorter, thicker, and curved as in digit I (m, o, t, w, y, and z). Digit V was also curved proximally (m-p, v, and x-z). The hind limb exhibited abnormalities in the tibia and fibula (q and r). Arrows indicate abnormal limb formations. Arrowheads indicate the fibular abnormality. *; interosseous space. R, radius; U, ulnar; T, tibia; F, fibula. Scale bars: 10 μm.

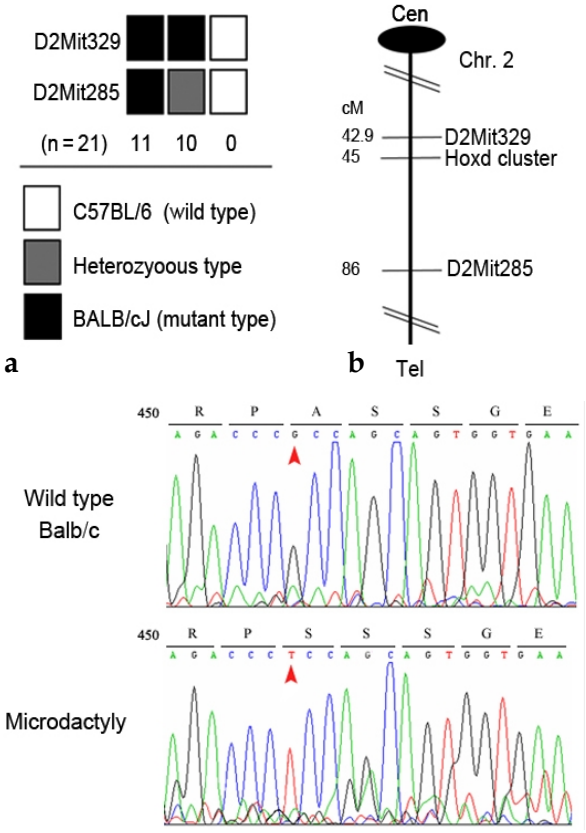

Fig. 2. Haplotype analysis and the genetic linkage map (a, b), and (c) mutation analysis of ENU-induced microdactyly mice. (a) Haplotype analysis of intraspecific backcross between mutant and C57BL/6. The (mutant × B6) F1 was crossed with (F1 × mutant) F2 and produced 21 mutant homozygous mice. Each column represents a chromosomal haplotype identified in the intercross and inherited from the F1 parents. Each genotype was determined by a single sequence length polymorphism. Black boxes, BALB/cJ alleles; white boxes, C57BL/6 alleles; grey boxes, both alleles. Markers are indicated on the left. (b) Genetic linkage map. (c) Sequencing of PCR products of WT and ENU-induced microdactyly mice. Red arrowheads indicate the mutations responsible for the phenotypes. Sequencing of Hoxd12 in ENU-induced microdactyly mice revealed G-to-T transversion at nucleotide 453, resulting in a change from alanine to serine.

Table 2. Gene-specific Primers for RT-qPCR

	Forward	Reverse
GAPDH	CTGGAGAAACCTGCCAAGTATG	ACCAGGAAATGAGCTTGACAAA
Bmp2	CCAAGAGACAT GTGAGGATT	AAGTCCACATACAAAGGGTG
Bmp4	TGCAGACCCTAGGTC AACTCT	AATTTTTCAACACCACCTTG
En1	CCTGGGTCTACTGCACACG CTAT	GGAACTCCGCCTTGAGTCTCTG
Gli3	TGGACTTGGCACCA ATGGAA	GGACCCTTGAATCCCTGTACCAC
Fgf4	CTTCGTGGCTATGAGCAG CAG	CGTAGGCTTCGTAGGCGTTGTA
Fgf8	CATCCGGACCTACCAGC TCTACA	AGTATCGGTCTCCACAATGAGCTTC
Lmx1b	TTGGACGGCATCAA GATGGA	TGCCAGGACGACTCGTTGAC
Ptch1	CATGCCAG AGACCAGGC TGA	GTCTCGTAGGCCGTTGAGGTAGAA
Shh	ATGTTTCTGGTGAT CCTTG	TACGTTGGGA ATAAACTGCT

RT-qPCR, quantitative real-time PCR.

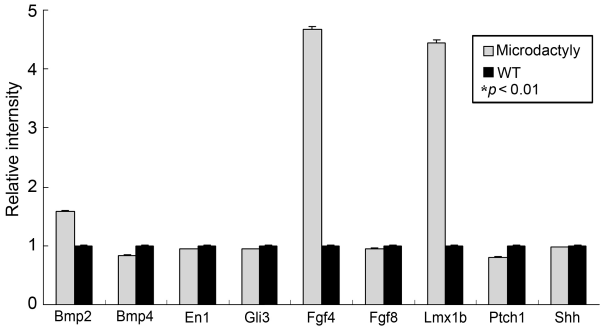

Fig. 3. Comparison of mRNA expression levels between ENU-induced microdactyly and WT (BALB/cJ) adult mice. Bmp2, Bmp4, En1, Gli3, Fgf4, Fgf8, Lmx1b, Ptch1 and Shh were detected in mictodactyly and WT mice. The expressions of Fgf4 and Lmx1b were significantly higher in microdactyly than in WT mice. The gene expression was normalized to that of the housekeeping gene, GAPDH. Data are mean and SD values (n=6). $*p < 0.01$.

sion levels of Gli3 and Shh were not changed in point mutated Hoxd12 mice (Fig. 3).

DISCUSSION

ENU mutagenesis is an effective strategy for developing mice models of human disease by inducing mutations that lead to unique phenotypes for gene-targeted strategies. Moreover, mutant phenotypes associated with point mutations might be more appropriate as models of human inherited disorders, since these are predominantly associated with changes to single base pairs.[15] Furthermore, mutagenesis screening represents an alternate source of mutant phenotypes for investigations.[16]

In limbs, Hoxd12 transcripts are absent from the intermediate segments, the presumptive zeugopods in both fore and hind limbs, with especially Hoxd12 being unaffected both in the proximal/posterior domain and in the future digit area.[17] In our ENU screening, we identified the phenotype, resulting from a point mutation in the Hoxd12 gene. Targeted mutagenesis of individual and multiple 5' Hoxd genes alter the size, shape, and number of bones, and delay chondrification and ossification.[18,19] Thus, these genes determine region-specific growth and differentiation in limb skeletal elements, acting in a combinatorial fashion during both early and late developmental stages.[20] The ENU-induced Hoxd12 mutation produces a distinct autosomal recessive phenotype of short digits and limbs, and crosstalk between factors such as Hoxd12, Bmps, Fgfs, and Shh during limb development is critical to correct digit formation.[4,5,8,21,22] Our mouse model could help understand the specific roles of Hoxd12. We identified the Hoxd12 point mutation involving G-to-T mutation at nucleotide 453, resulting in a change from alanine to serine (Fig. 2). Our analysis revealed that the function of the mutated Hoxd12 protein at the

molecular level might affect protein structure and DNA binding, which would be altered by Hodx12 translational events such as changes in the transcription rate or mRNA stability.

There are striking similarities between microdactyly and Hoxd12-knock-out mice. Digits II and V were short in Hoxd12-knock-out mice, in which exon 2 was deleted.[23] Digit II was strongly affected and the wrist carpal bone showed a subtle, characteristic indentation at its distal border. In addition, digit V of these mice was also twisted proximally, as in microdactyly mice.[23] Moreover, Hoxd12 misexpression caused a posterior transformation, duplications of the distal anterior skeletal elements, and selective reductions in specific proximal limb elements.[24] The Hoxd proteins also reversed the Gli3-repressor function by acting downstream of Shh, thereby promoting digit formation.[25]

Fgf4 influences digit morphogenesis, which correlates with the widespread changes in gene expression, also affecting the posterior members of the Hoxd.[26] Hoxd12 and Hoxd13 were consistently induced in the anterior-distal limb mesenchyme, accompanying mirror-image duplication of the digit pattern.[27] In order to elucidate Hoxd12 function, we examined factors involved in digit formation, which included Bmp2, Bmp4, En1, Gli3, Fgf4, Fgf8, Lmx1b, and Ptch1.[9,28,29] Only Fgf4 and Lmx1b were found to be significantly increased in microdactyly mice (Fig. 3). Fgf4 is the earliest member of the fibroblast growth factor (FGF) family identified, and is expressed during embryogenesis where it plays an essential role in post implantation development, limb growth, and patterning.[30] In addition, increased FGF signaling occurs when the Fgf4 gain-of-function allele is activated in a WT limb bud. Excess Fgf4 causes supernumerary posterior digit (postaxial polydactyly) formation and cutaneous syndactyly between all the digits.[31] These observations underscore the importance of controlling FGF expression during normal limb development. Lmx1b is involved in dorsal-ventral patterning and may play additional roles in anterior-posterior patterning and growth.[28]

In the resesent study, the mutation appeared to be more severe than the full knockout reported previously by two groups. We described the analysis of ENU-mutated mice showing a digit phenotype and the identification of a point mutation within the Hoxd12 gene, causing a serine to alanine substitution. Moreover, we observed perturbation of the expression of some genes in mutant mice that play relevant roles in limb development. It is not clear how these abnormalities are related to the increases of Fgf4 and Lmx1b expressions in the mutant mouse. One possibility is that a point mutation rather than the entire deletion of Hoxd12, such as knockout and transgenic mice, causes the abnormal limb phenotype. This discrepancy could reflect the differential phenotypic effects of changes on single amino acids and be useful in phenotype screening to detect mutants. The precise nature of the spectrum of differences obviously requires further investigation.

REFERENCES

1. Balling R. ENU mutagenesis: analyzing gene function in mice. Annu Rev Genomics Hum Genet 2002;2:463-92.
2. Clark AT, Bertram JF. Advances in renal development. Curr Opin Nephrol Hypertens 2000;9:247-51.
3. Godinho SI, Nolan PM. The role of mutagenesis in defining genes in behaviour. Eur J Hum Genet 2006:14: 651-9.
4. Niswander L. Pattern formation: old models out on a limb. Nat Rev Genet 2003;4:133-43.
5. Tickle C. Patterning systems--from one end of the limb to the other. Dev Cell 2003;4:449-58.
6. Chiang C, Litingtung Y, Harris MP, Simandl BK, Li Y, Beachy PA, et al. Manifestation of the limb prepattern: limb development in the absence of sonic hedgehog function. Dev Biol 2001;236:421-35.
7. Kraus P, Fraidenraich D, Loomis CA. Some distal limb structures develop in mice lacking Sonic hedgehog signaling. Mech Dev 2001;100:45-58.
8. Sanz-Ezquerro JJ, Tickle C. Digital development and morphogenesis. J Anat 2005;202:51-8.
9. Zhu J, Nakamura E, Nguyen MT, Bao X, Akiyama H, Mackem S. Uncoupling Sonic hedgehog control of pattern and expansion of the developing limb bud. Dev Cell 2008;14:624-32.
10. Zákány J, Kmita M, Duboule DA. A dual role for Hox genes in limb anterior-posterior asymmetry. Science 2004;304:1669-72.
11. Tarchini B, Duboule D. Control of Hoxd genes' collinearity during early limb development. Dev Cell 2006; 10:93-103.
12. Galis F, Kundrát M, Metz JA. Hox genes, digit identities and the theropod/bird transition. J Exp Zoolog B Mol Dev Evol 2005;304:198-205.
13. Pera EM, Ikeda A, Eivers E, De Robertis EM. Integration of IGF, FGF, and anti-BMP signals via Smad1 phos-

phorylation in neural induction. Genes Dev 2003;17: 3023-8.
14. Classical linkage analysis and mapping panels. In: Silver LM, editor. Mouse genetics: concepts and applications. New York: Oxford University Press; 1995. p.195-263.
15. Quwailid MM, Hugill A, Dear N, Vizor L, Wells S, Horner E, et al. A gene-driven ENU-based approach to generating an allelic series in any gene. Mamm Genome 2004;15:585-91.
16. Patton EE, Zon LI. The art and design of genetic screens: zebrafish. Nat Rev Genet 2001;2;956-66.
17. Hérault Y, Beckers J, Kondo T, Fraudeau N, Duboule D. Genetic analysis of a Hoxd-12 regulatory element reveals global versus local modes of controls in the HoxD complex. Development 1998;125:1669-77.
18. Rijli FM, Chambon P. Genetic interactions of Hox genes in limb development: learning from compound mutants. Curr Opin Genet Dev 1997;7:481-7.
19. Zákány J, Duboule D. Synpolydactyly in mice with a targeted deficiency in the HoxD complex. Nature 1996; 384:69-71.
20. Caronia G, Goodman FR, McKeown CM, Scambler PJ, Zappavigna V. An I47L substitution in the HOXD13 homeodomain causes a novel human limb malformation by producing a selective loss of function. Development 2003;130:1701-12.
21. Dillon R, Gadgil C, Othmer HG. Short- and long-range effects of Sonic hedgehog in limb development. Proc Natl Acad Sci U S A 2003;100:10152-7.
22. Drossopoulou G, Lewis KE, Sanz-Ezquerro JJ, Nikbakht N, McMahon AP, Hofmann C, et al. A model for anteroposterior patterning of the vertebrate limb based on sequential long- and short-range Shh signalling and Bmp signalling. Development 2000;127:1337-48.
23. Davis AP, Capecchi MR. A mutational analysis of the 5' HoxD genes: dissection of genetic interactions during limb development in the mouse. Development 1996; 122:1175-85.
24. Knezevic V, De Santo R, Schughart K, Huffstadt U, Chiang C, Mahon KA, et al. Hoxd-12 differentially affects preaxial and postaxial chondrogenic branches in the limb and regulates Sonic hedgehog in a positive feedback loop. Development 1997;124:4523-36.
25. Chen Y, Knezevic V, Ervin V, Hutson R, Ward Y, Mackem S. Direct interaction with Hoxd proteins reverses Gli3-repressor function to promote digit formation downstream of Shh. Development 2004;131: 2339-47.
26. Ngo-Muller V, Muneoka K. Influence of FGF4 on digit morphogenesis during limb development in the mouse. Dev Biol 2000;219:224-36.
27. Wada N, Kawakami Y, Nohno T. Sonic hedgehog signaling during digit pattern duplication after application of recombinant protein and expressing cells Dev Growth Differ 1999;41:567-74.
28. Chen H, Johnson RL. Interactions between dorsal-ventral patterning genes lmx1b, engrailed-1 and wnt-7a in the vertebrate limb. Int J Dev Biol 2002;46:937-41.
29. Omi M, Fisher M, Maihle NJ, Dealy CN. Studies on epidermal growth factor receptor signaling in vertebrate limb patterning. Dev Dyn 2005;233:288-300.
30. Sun X, Mariani FV, Martin GR, Functions of FGF signalling from the apical ectodermal ridge in limb development. Nature 2002;418:501-8.
31. Lu P, Minowada G, Martin GR. Increasing Fgf4 expression in the mouse limb bud causes polysyndactyly and rescues the skeletal defects that result from loss of Fgf8 function. Development 2006;133:33-42.